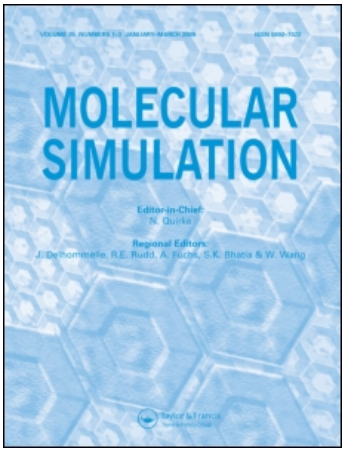

Molecular Simulation
Publication details, including instructions for authors and subscription information:
http://www.informaworld.com/smpp/title~content=t713644482

Optimisation of multiple time-step hybrid Monte Carlo Wang-Landau simulations in the isobaric-isothermal ensemble for the determination of phase equilibria

C. Desgranges[a]; E. A. Kastl[a]; T. Aleksandrov[a]; J. Delhommelle[a]
[a] Department of Chemistry, University of North Dakota, Grand Forks, ND, USA

Online publication date: 03 August 2010

To cite this Article Desgranges, C. , Kastl, E. A. , Aleksandrov, T. and Delhommelle, J.(2010) 'Optimisation of multiple time-step hybrid Monte Carlo Wang-Landau simulations in the isobaric-isothermal ensemble for the determination of phase equilibria', Molecular Simulation, 36: 7, 544 — 551
To link to this Article: DOI: 10.1080/08927021003762738
URL: http://dx.doi.org/10.1080/08927021003762738

Molecular Simulation
Vol. 36, Nos. 7–8, June–July 2010, 544–551

Taylor & Francis
Taylor & Francis Group

Optimisation of multiple time-step hybrid Monte Carlo Wang–Landau simulations in the isobaric–isothermal ensemble for the determination of phase equilibria

C. Desgranges, E.A. Kastl, T. Aleksandrov and J. Delhommelle*

Department of Chemistry, University of North Dakota, 151 Cornell Street Stop 9024, Grand Forks, ND 58202, USA

(*Received 8 January 2010; final version received 9 March 2010*)

We discuss the optimisation as well as the convergence of a recently developed molecular simulation method using a Wang–Landau sampling scheme, combined with multiple time-step hybrid Monte Carlo (MC) simulations in the isothermal–isobaric ensemble, to determine vapour–liquid equilibria. This method has the advantage of being simple to use, as only a single simulation run at a given temperature directly gives the coexistence properties, and of being transferable to any kind of fluid, since the method is readily applicable to any molecular architecture. We apply this method to two branched alkanes, isopentane and isobutane, and discuss how we optimise the various simulation parameters. The vapour–liquid coexistence curve as well as the critical point obtained in this work are in excellent agreement with those found experimentally and in previous work using a combination of the Gibbs ensemble MC method with the configurational bias technique.

Keywords: Wang–Landau sampling; phase equilibria; hybrid Monte Carlo; branched alkanes

1. Introduction

The determination of vapour–liquid equilibria is of key importance for many applications, particularly in the field of petrochemistry. There has been a lot of interest in designing a simple and robust molecular simulation method applicable to all fluids, ranging from simple to complex molecules. In the last two decades, the Gibbs ensemble Monte Carlo (GEMC) [1] method has become a popular method to determine the liquid–vapour coexistence curve as well as the critical properties of a wide variety of fluids, including those of simple model fluids such as the Lennard-Jones fluid [1], of metals such as aluminium [2], of small molecules such as carbon dioxide [3] or hydrogen sulphide [4–7] and of chain molecules such as alkanes [8–14], ethers and ketones [15] or sulphides [16]. The GEMC method uses two simulation boxes simulating the vapour and liquid phases, respectively. The different moves allowed during a GEMC simulation are the translation of atoms/molecules, volume changes of the simulation boxes and transfer of atoms/molecules from one phase to the other. These moves allow the system to reach the equilibrium (same pressure, chemical potential and temperature for the two phases) at a given temperature. The limitation of this method stems from the fact that the probability of acceptance for transfer moves becomes very low for liquid densities. Several techniques have been implemented to overcome this difficulty. Using the cavity bias [17] and the configurational bias [18], simulations of the vapour–liquid equilibria were achieved for *n*-alkanes [14], linear and branched alkanes [8–14], and squalane [19–22]. However, these techniques rely on the implementation of a specific bias, function of the molecular architecture of the system studied, which may not be valid and efficient for other types of molecular fluids. For instance, the configurational bias move, introduced for linear alkanes, was shown to be invalid for branched alkanes and a modified version of this move had to be implemented for branched alkanes [23]. However, despite its drawbacks, the configurational bias method has remained a key ingredient of the recently developed flat histogram methods for the phase equilibria of alkanes, such as the grand-canonical transition matrix MC methods [24,25].

In this paper, we use a recently developed approach based on a Wang–Landau sampling [26–31], combined with hybrid MC (WL-HMC) simulations in the isothermal–isobaric ensemble, to determine vapour–liquid equilibria. The aim of the WL-HMC approach is to provide a simple and general method to calculate the phase equilibria for complex molecules. Similarly to the GEMC approach, no prior knowledge of the thermodynamics of the system is needed. In particular, no guess value for the pressure or chemical potential of coexistence is required. In addition, a single simulation is required to obtain the coexistence properties at a given temperature. However, unlike in the GEMC method, we use a single simulation box, whose volume varies throughout the simulation to allow for a uniform sampling of all (liquid

*Corresponding author. Email: jdelhommelle@chem.und.edu

ISSN 0892-7022 print/ISSN 1029-0435 online

DOI: 10.1080/08927021003762738
http://www.informaworld.com

and vapour) densities, to calculate the coexistence properties of the molecule studied. This circumvents the issue occurring in GEMC of transferring molecules from one phase to the other (or the issue of inserting molecules in grand-canonical transition matrix methods), and therefore removes the need for any cavity bias or configurational bias technique. In the recent paper, we applied this approach to different systems, including the Lennard-Jones fluid [32] (see also Ref. [33]), benzene [32], copper [34] and, more recently, polyaromatic hydrocarbons [35] and demonstrated the reliability and accuracy of this method. The aim of this work is to discuss several technical aspects of this approach, including the implementation and optimisation of a multiple time-step HMC simulations to integrate fast and slow motions in molecular fluids as well as the criteria for convergence of the WL-HMC method.

This paper is organised as follows. In the first part, we detail how one can implement the WL-HMC method in the NPT ensemble. We define the acceptance rules for the molecular dynamics and volume changes moves, which are the only two moves considered in this method. We then show how we extract the canonical partition function of the system by analysing the WL-HMC simulation results and obtain the coexistence properties. In the second part, we apply this method to determine the vapour–liquid equilibria of isobutane and isopentane. In particular, we discuss the optimisation of the simulation parameters as well as the convergence of the WL-HMC simulations. We then compare our results to those found experimentally and in previous simulations and draw our main conclusions in the last section.

2. Implementation of the method

In this section, we present the different steps used to implement a WL sampling associated with a HMC in the isothermal–isobaric ensemble. We use two different moves: long molecular dynamics (MD) trajectories (which allow the system to relax between two different moves) and volume changes (which allow us to sample all the volume's interval). We define the acceptance rules for these moves below. At the end, when the simulation has converged, we show how we obtain a smooth and accurate estimate of the canonical partition function $Q(N, V, T)$. Then, we use this estimate of $Q(N, V, T)$ to calculate the densities for the two coexisting phases. Finally, we obtain an estimate for the critical point by applying a density scaling law and the law of rectilinear diameters.

2.1 MD moves

We implement a HMC method [32] instead of combining the WL sampling with a conventional MC [33]. We replace the random translation and rotation moves used in conventional MC by a long MD trajectory. It permits the system to relax along a long MD trajectory (see our previous paper using HMC simulations for more detail [36–40]). The probability of accepting a MD trajectory from an old configuration o to a new configuration n is given by:

$$\mathrm{acc}(o \to n) = \min\left[1, \exp\left(-\frac{(E(n) - E(o))}{k_B T}\right)\right], \quad (1)$$

where E is the total energy, i.e. the sum of the potential and kinetic energy for the system.

In HMC simulations, the integrator must satisfy the time-reversible and area-preserving properties [41,42]. We choose to implement the multiple time-step RESPA-NVE algorithm [43] to integrate the equations of motion since this algorithm is time-reversible and area-preserving.

2.2 Volume changes moves

The second type of move consists in random volume changes for the whole system. As the order parameter for the vapour–liquid transition is density, we choose to perform a uniform sampling of the volume V for a fixed number of molecules in the isothermal–isobaric ensemble. In order to achieve a uniform sampling of V [33], we introduce a bias distribution, $p_{\mathrm{bias}}(\Gamma,V)$, function of a given configuration Γ and of the volume V as

$$p_{\mathrm{bias}}(\Gamma, V) = \frac{V^N \exp\left[-(U(\Gamma)/k_B T)\right]}{N!\Lambda^{3N} Q(N, V, T)}, \quad (2)$$

where N is the number of molecules, Λ is the De Broglie wavelength and $Q(N, V, T)$ is the canonical partition function.

We then obtain the probability of accepting a volume change move from an old configuration o with (Γ_o,V_o) to a new configuration n with (Γ_n,V_n):

$$\mathrm{acc}(o \to n) = \min\left[1, \frac{Q(N, V_o, T)}{Q(N, V_n, T)} \frac{V_n^N \exp\left(-(U(\Gamma_n)/k_B T)\right)}{V_o^N \exp\left(-(U(\Gamma_o)/k_B T)\right)}\right]. \quad (3)$$

We note that the pressure does not appear in Equation (3) and that the biasing function needed to perform a uniform sampling of V is the canonical partition function at N, V and T fixed.

2.3 Determination of the canonical partition function

The aim of this method is to obtain an accurate estimate for the canonical partition function. The first step is to determine the upper and lower bounds for the volume

that we have to visit in order to find the coexistence properties of our system at a given temperature. These values can be found either in the literature or can be evaluated by shortened WL-HMC simulations (using a larger convergence factor, see below). We then divide this subset of volume into different uniform intervals of $\ln V$ instead of V for more convenience during the sampling (this changes Equation (3) only slightly as the factors of V^N are replaced by V^{N+1}). During our simulations, we consider two histograms. The first one collects the estimate for $Q(N,V,T)$ and the second one, $H(V)$, monitors the number of times a given interval of V is visited. At the beginning of the simulation, we give the same initial value to $Q(N,V,T)$ for all values of $\ln V$. We also introduce a convergence factor f which will allow us to control that we have a flat histogram. We start with an initial value of $\ln f = 1$. Whenever a given interval for $\ln V$ is visited, the value for the partition function is updated. $Q(N,V,T)$ is multiplied by f. Every time a given volume interval is visited, the value for $H(V)$ is also updated. When the histogram $H(V)$ is reasonably flat (in practice, it is accomplished when all intervals for the volume have been visited at least 500 times), the WL-HMC simulation has converged. We therefore reduce the value of convergence factor to $\sqrt{f}$, initialise all entries for the histogram $H(V)$ and start over a WL-HMC run with this new value for the convergence factor f. This procedure is repeated until $\ln f = 10^{-5}$.

2.4 Analysis of the simulation

Once the WL-HMC simulation has converged, we analyse our results. The first step consists in evaluating the volume distribution $p(V)$:

$$p(V) = \frac{Q(N,V,T)\exp(-PV/k_BT)}{Q(N,P,T)}, \tag{4}$$

where

$$Q(N,P,T) = \int_0^\infty Q(N,V,T)\exp(-PV/k_BT)\,dV, \tag{5}$$

$Q(N,P,T)$ is the isothermal–isobaric partition function. This allows to locate the bin number N_b as well as the volume V_b, corresponding to the minimum of the volume distribution and therefore to the boundary between the peak associated with the liquid and that associated with the vapour. We then calculate the probability Π_{liq} associated with the liquid phase according to

$$\Pi_{liq} = \int_0^{V_b} p(V)\,dV \tag{6}$$

and the probability Π_{vap} associated with the vapour phase by

$$\Pi_{vap} = \int_{V_b}^\infty p(V)\,dV. \tag{7}$$

The saturation pressure (P_{coex}) is defined as $\Pi_{liq} = \Pi_{vap}$. Once the saturation pressure P_{coex} is known, the densities for the two coexisting phases, i.e. for the vapour (ρ_{vap}) and for the liquid (ρ_{liq}), may be calculated:

$$\rho_{liq} = \frac{\int_0^{V_b}(N/V)V^N Q(N,V,T)\exp(-(P_{coex}V/k_BT))\,dV}{\int_0^{V_b} Q(N,V,T)\exp(-(P_{coex}V/k_BT))\,dV}$$
$$\rho_{vap} = \frac{\int_{V_b}^\infty(N/V)V^N Q(N,V,T)\exp(-(P_{coex}V/k_BT))\,dV}{\int_{V_b}^\infty Q(N,V,T)\exp(-(P_{coex}V/k_BT))\,dV}. \tag{8}$$

Finally, the critical point is estimated by fitting the WL-HMC results with a density scaling law to obtain the critical temperature T_c defined by:

$$\rho_l - \rho_v = B(T_c - T)^\beta, \tag{9}$$

where ρ_l and ρ_v are the densities of the liquid and vapour phases, respectively, $\beta = 0.3265$ is the 3D Ising order-parameter exponent and B is a fitting parameter. We then use this value of T_c to obtain the critical density ρ_c via the law of rectilinear diameters [44,45] given by:

$$\frac{\rho_l + \rho_v}{2} = \rho_c + A(T - T_c), \tag{10}$$

where A is a fitting parameter.

3. Application to two branched alkanes: isobutane and isopentane

3.1 Molecular model

We use the NERD (Nath, Escobedo and de Pablo revised) united-atom force field, introduced by Nath and de Pablo [8], to determine the phase equilibria of isobutane and isopentane. In this model, each CH_3, CH_2 and CH group is modelled by a single interaction site. The NERD potential consists of two terms, accounting for the intramolecular and the intermolecular interactions, respectively. First, the intramolecular part consists in describing the interactions between each site inside a molecule. It is written as the sum of a Lennard-Jones potential (between sites that are separated by more than three bonds):

$$U(r_{ij}) = 4\varepsilon\left[\left(\frac{r_{ij}}{\sigma}\right)^{12} - \left(\frac{r_{ij}}{\sigma}\right)^{6}\right], \tag{11}$$

a bond stretching potential,

$$\frac{U(r_{ij})}{k_B} = \frac{K_r}{2}(r_{ij} - b_{eq})^2, \tag{12}$$

a bond bending potential,

$$\frac{U(\theta)}{k_B} = \frac{K_\theta}{2}(\theta - \theta_{eq})^2, \tag{13}$$

and a torsional potential,

$$\frac{U(\theta)}{k_B} = V_0 + V_1(1 + \cos\phi) + V_2(1 - \cos 2\phi) + V_3(1 + \cos 3\phi). \tag{14}$$

The second part of the potential is the intermolecular potential describing the interactions between two different molecules. It is modelled by a Lennard-Jones potential (see Equation (11)).

The parameters for the two systems studied in this paper are given in Tables 1–3. For all the simulations, we use a cut-off radius of 10 Å. Beyond this cut-off, we apply the standard long-range corrections [46]. In addition, we use the Lorentz–Berthelot rules [46,47] to determine the parameters between pairs of unlike interaction sites:

$$\sigma_{ij} = \frac{1}{2}(\sigma_{ii} + \sigma_{jj}), \tag{15}$$

$$\varepsilon_{ij} = (\varepsilon_{ii}\,\varepsilon_{jj})^{1/2}. \tag{16}$$

3.2 *Optimisation of the simulation parameters*

We carry out simulations with a system size of 108 molecules for the two branched alkanes studied. As with the GEMC method, no prior knowledge of the thermodynamic properties of the system is required. One only needs to specify reasonable values for the input temperature, i.e. below the critical temperature, and for the range of densities, encompassing the vapour and liquid phases, sampled during the volume changes. The upper and lower bounds for the volume are chosen to correspond to densities of 0.006 and 0.6 g cm^{-3}. The WL-HMC simulation consists of two types of MC moves, i.e. MD trajectories, accounting for half of the attempted random moves, and random volume changes, accounting for the other half of the attempted random moves. For all systems, the MD trajectories were integrated from initial velocities drawn from a Gaussian distribution. As noted above, we implement the multiple time-step RESPA-NVE algorithm [43] to integrate the equations of motion since this algorithm is time-reversible and area-preserving. There is considerable freedom in choosing the values for the time steps for the fast (intramolecular) motions and the slow (intermolecular) motions, as well as in the length of the MD trajectory. In line with what is usually done in regular MC simulations [46], we set the three parameters of the simulations (the two time steps and the length of the MD trajectory) so that the probability of acceptance for the MD trajectory is 50%. For this purpose, for each set of parameters, we run for a single temperature a shortened version WL-HMC simulation, i.e. a sweep of all densities for a single value of the convergence factor (we choose $f = e$, the initial value of the convergence factor). The set of parameters we select is the set that gives probabilities of acceptance of about 50%. This is achieved with, in the case of isobutane, a MD trajectory of 20 steps with a 19.3 fs time step for the slow modes (the 'fast' intramolecular motions being integrated 800 times over the time step of 19.3 fs, i.e. over a time step of 19.3/800 = 0.024125 fs), and, in the case of isopentane, a MD trajectory of 20 steps with a 16.9 fs time step for the slow modes (the 'fast' intramolecular motions being integrated 700 times over the time step of 16.9 fs, i.e. over a time step of 19.3/800 = 0.024143 fs). For both systems, the other type of random move consists of random volume changes, with a maximum volume change equal to twice the bin width of the histogram. We plot, in Figures 1 and 2, the acceptance probability for both MD trajectories and volume change moves for isobutane and isopentane, respectively. We find that the lowest acceptance probability is obtained for the smallest volume bin. As shown in Figures 1 and 2, the acceptance probability is very close to 50% for both the MD moves and volume change moves, demonstrating that the parameters selected here allow for efficient WL-HMC simulations.

Table 1. Parameters for the Lennard-Jones potential [8].

	σ_{CH_3} (Å)	ε_{CH_3} (K)	σ_{CH_2} (Å)	ε_{CH_2} (K)	σ_{CH} (Å)	ε_{CH} (K)
Isobutane	3.88	78.23	–	–	3.85	39.7
Isopentane	3.90	79.5	3.93	45.8	3.85	39.7

Table 2. Parameters for the bond stretching and bending potentials [8].

K_r (K Å^{-2})	b_{eq} (Å)	K_θ (K rad^{-2})	θ_{eq} (°)	θ_{eq} (°) (centred at a CH unit)
96,500	1.54	62,500	114.0	109.4

Table 3. Parameters for the torsional potential [8].

V_0 (K)	V_1 (K)	V_2 (K)	V_3 (K)
1416.3	398.3	139.12	−901.2

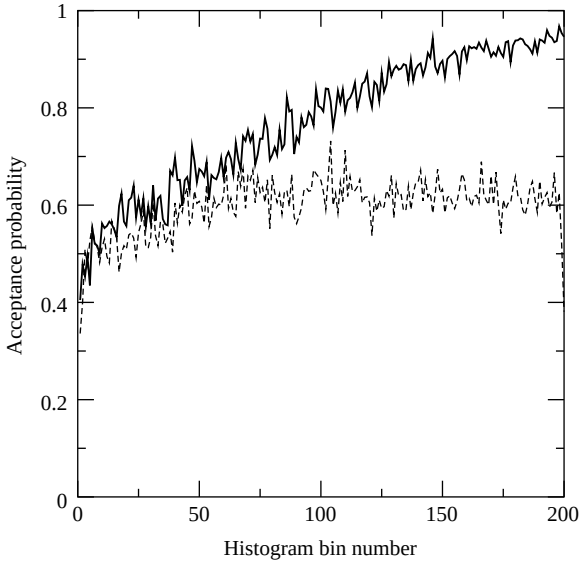

Figure 1. Acceptance probability of the two types of HMC moves for isobutane at $T = 300\,\mathrm{K}$ (solid line, MD moves; dashed line, volume change moves).

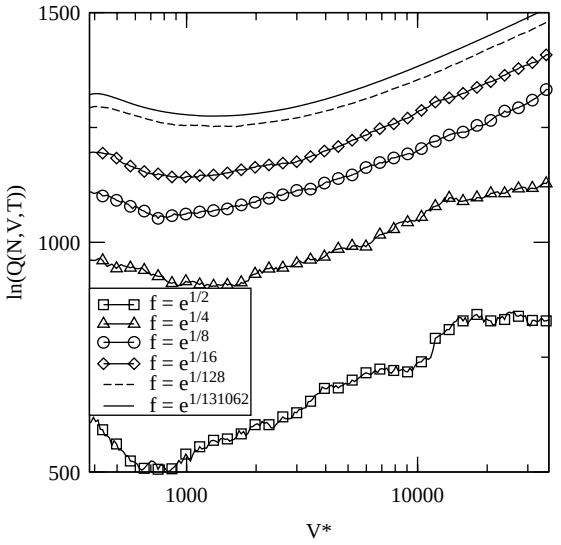

Figure 3. Evolution of the estimate of the canonical partition function as a function of the reduced volume along a NPT HMC-WL simulation for isobutane at $T = 350\,\mathrm{K}$.

3.3 Criterion for the convergence of the WL-HMC method

The key point is to obtain an accurate estimate for the canonical partition function, $Q(N, V, T)$, at the end of the WL-HMC simulations. We plot in Figure 3, the running estimate of $\ln(Q(N, V, T))$ against the reduced volume V^* for different values of the convergence factor f for a system of 108 isobutane molecules at $T = 350\,\mathrm{K}$. As the WL-HMC simulations advance, the running estimate for $\ln(Q(N, V, T))$ becomes smoother and smoother. This can best be seen by evaluating numerically the derivative of the running estimate of $\ln(Q(N, V, T))$ with respect to V^* (see Figure 4). Figure 4 shows that, for large values of the convergence factor f, there is a high level of noise for this derivative (corresponding to the rough curves for $\ln(Q(N, V, T))$ shown in Figure 3), while, at the end of the WL-HMC simulation, the derivative is a continuous, essentially noise-free, function (corresponding to the

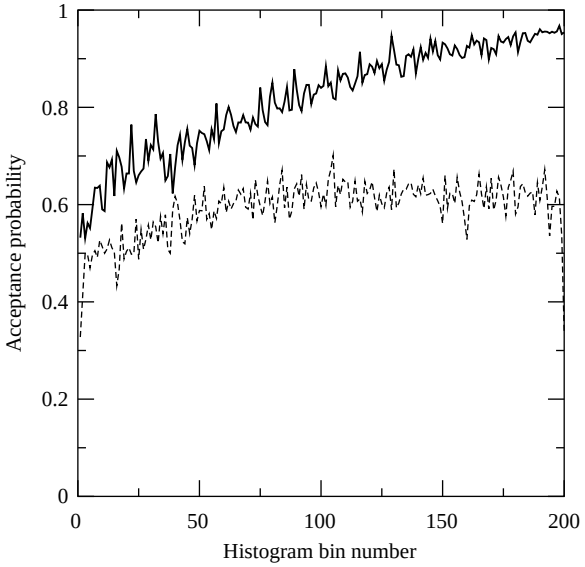

Figure 2. Acceptance probability of the two types of HMC moves for isopentane at $T = 350\,\mathrm{K}$ (solid line, MD moves; dashed line, volume change moves).

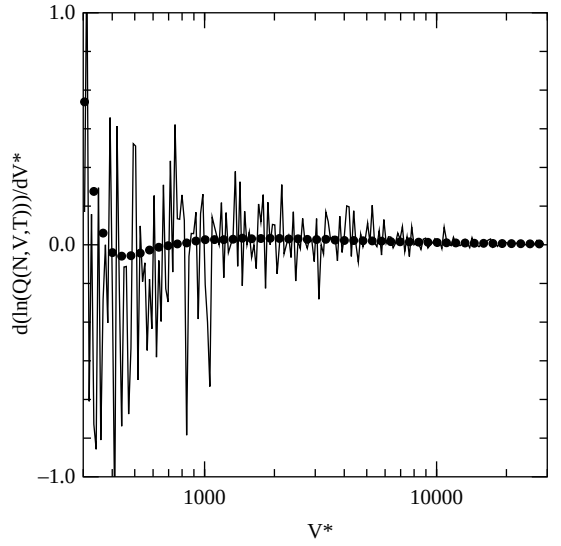

Figure 4. Derivative of the logarithm of the running estimate for the canonical partition function with respect to volume for isobutane at $T = 350\,\mathrm{K}$ (solid line, $f = \sqrt{\mathrm{e}}$; filled circles, $f = \mathrm{e}^{1/2^{16}}$).

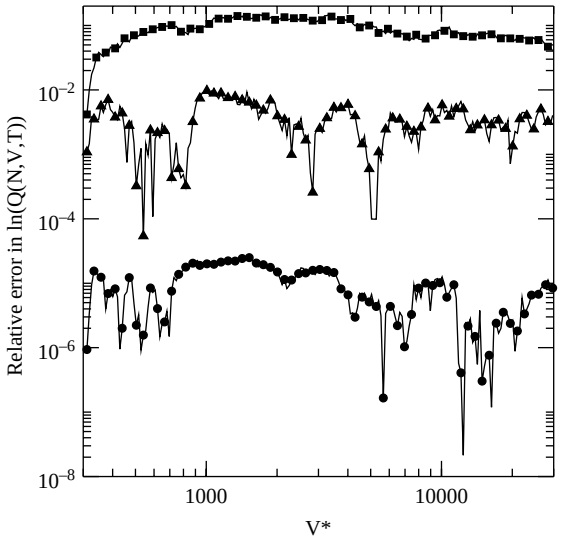

Figure 5. Relative error in the logarithm of the running estimate for the canonical partition function for isobutane at $T = 350\,\mathrm{K}$ (ΔE_2, squares; ΔE_6, triangles; ΔE_16, circles).

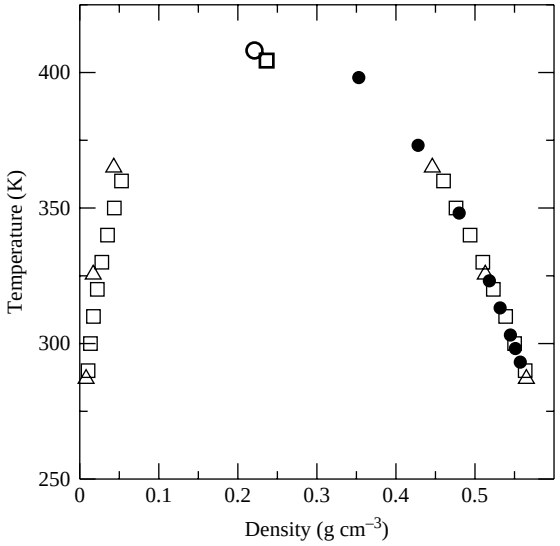

Figure 6. Vapour–liquid equilibria for isobutane obtained from NPT WL-HMC simulations (open squares), experiments [48] (filled circles) and Nath and de Pablo [8] simulations (open triangles). The bold symbols represent the critical point.

smooth curve for $\ln(Q(N,V,T))$ shown in Figure 3). To better quantify that the WL-HMC have converged, we define the following function:

$$\Delta E_n = \left| \frac{\ln Q_{f_n}(N,V,T) - \ln Q_{f_{n-1}}(N,V,T)}{\ln Q_{f_n}(N,V,T)} \right|, \qquad (17)$$

where $Q_{f_n}(N,V,T)$ is the running estimate for the canonical partition function for a factor of convergence $f_n = \mathrm{e}^{1/2^n}$. ΔE_n may be interpreted as the relative error made for a convergence factor of $f_n = \mathrm{e}^{1/2^n}$. It is also a measure of the convergence of the WL-HMC simulations. Figure 5 shows various values of ΔE_n, collected during the course of the WL-HMC simulations. Figure 5 establishes that the WL-HMC simulations converge since the relative error steadily decreases as the convergence factor increases. At the end of the WL-HMC simulations (for ΔE_{16} or, in other words, right before $\ln f < 10^{-5}$ in the simulations), the relative error is less than 10^{-4} for all values of V^* and the WL-HMC simulations are deemed to have converged.

3.4 Results and discussion

We carry out WL-HMC simulations for eight temperatures ranging from $T = 290$ to $360\,\mathrm{K}$ for isobutane and from $T = 340$ to $410\,\mathrm{K}$ for isopentane. Once we have a good estimate of the partition function for each temperature, we are able to calculate the densities of the liquid and vapour phases at coexistence (see Equation (8)). We present, in Figures 6 and 7, the vapour–liquid equilibria for isobutane and isopentane, respectively, together with data obtained from experiments [48] and from previous simulations using the GEMC method, combined with the configurational bias technique [8]. Figures 6 and 7 show that our results, obtained with WL-HMC simulations, are in excellent agreement with the available experimental data as well as with previous simulation work [8]. We then calculate the critical density and temperature using Equations (9) and (10). For isobutane, we obtain a critical temperature $T_c = 404 \pm 8\,\mathrm{K}$ and a critical density $\rho_c = 236 \pm 15\,\mathrm{kg/m^3}$. Experimental data [48] give a

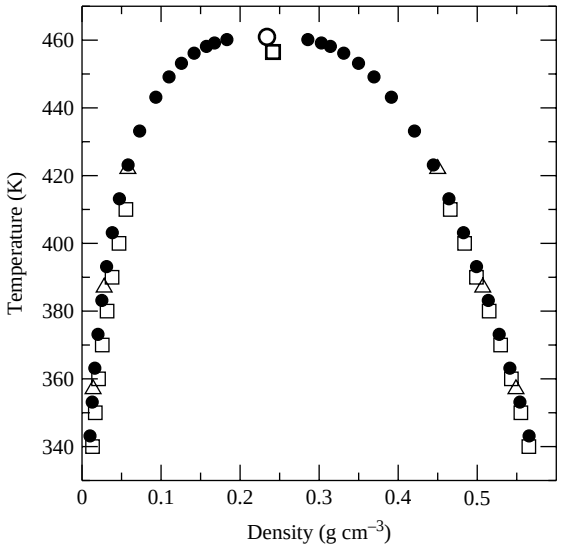

Figure 7. Vapour–liquid equilibria for isopentane obtained from NPT WL-HMC simulations (open squares), experiments [48] (filled circles) and Nath and de Pablo [8] simulations (open triangles). The bold symbols represent the critical point.

critical temperature $T_c = 408.13\,\mathrm{K}$ and a critical density $\rho_c = 221\,\mathrm{kg/m^3}$. The estimate for the critical temperature, extrapolated from the WL-HMC results, is within 1% of the experimental critical temperature and the estimate for the critical density is within 7% of the experiment for isobutane. For isopentane, we find a critical temperature of $T_c = 457 \pm 8\,\mathrm{K}$ and a critical density of $\rho_c = 241 \pm 15\,\mathrm{kg/m^3}$, respectively. These values have to be compared with those obtained from experiments for which $T_c = 460.95\,\mathrm{K}$ and $\rho_c = 234\,\mathrm{kg/m^3}$ [48]. Our estimates for the critical temperature and critical density differ from the experimental data by only 1 and 3%. The densities for the two coexisting phases, obtained from the WL-HMC simulations, as well as the critical points for isobutane and isopentane, extrapolated from the WL-HMC simulations, are therefore in excellent agreement with the experimental data. This excellent agreement demonstrates the reliability and accuracy of the WL-HMC approach presented in this paper. We finally add that the advantage of the WL-HMC simulations in the isothermal–isobaric ensemble is its generality, i.e. its ability to accurately predict the phase equilibria of any molecular fluids. This is unlike other methods, such as the GEMC method or the grand-canonical transition matrix, requiring the use of configurational bias moves, which need to be tailored to the molecular architecture of the studied fluid [23].

4. Conclusion

In this work, we detail how we implement a WL sampling with multiple time-step HMC simulations in the isothermal–isobaric ensemble and apply this algorithm to determine the phase equilibria of branched alkanes. We show that this method is simple and general since it can be applied as is to any system as no additional bias moves, dependent on the molecular architecture, is required. As with the GEMC method, no prior knowledge of the thermodynamics of the system (e.g. coexisting pressure or chemical potential) and only a single simulation at a given temperature is required to calculate the coexistence properties of a system. With the example of two branched alkanes, we discuss how we optimise the simulation parameters and how we analyse and quantify the convergence of the WL-HMC simulations. The resulting coexisting densities, as well as the extrapolated critical point, we obtain for isobutane and isopentane, are in excellent agreement with the available experimental data and previous simulation work using the GEMC method, thereby establishing the reliability and accuracy of the method proposed in this paper.

Acknowledgement

Financial support from ND EPSCoR through the NSF Grant EPS-0814442 is gratefully acknowledged.

References

[1] A.Z. Panagiotopoulos, *Direct determination of phase coexistence properties of fluids by Monte Carlo simulation in a new ensemble*, Mol. Phys. 61 (1987), pp. 813–816.
[2] D. Bhatt, A.W. Jasper, N.E. Schultz, J.I. Siepmann, and D.G. Truhlar, *Critical properties of aluminum*, J. Am. Chem. Soc. 128 (2006), pp. 4224–4225.
[3] J.G. Harris and K.H. Yung, *Carbon dioxide's liquid–vapor coexistence curve and critical properties as predicted by a simple molecular model*, J. Phys. Chem. 99 (1995), pp. 12021–12024.
[4] T. Kristof and J. Liszi, *Effective intermolecular potential for fluid hydrogen sulfide*, J. Phys. Chem. B 101 (1997), pp. 5480–5483.
[5] J. Delhommelle, A. Boutin, and A.H. Fuchs, *Molecular simulation of vapour–liquid coexistence curves for hydrogen sulfide–alkane and carbon dioxide–alkane mixtures*, Mol. Simul. 22 (1999), pp. 351–368.
[6] J. Delhommelle, P. Millie, and A.H. Fuchs, *On the role of the definition of potential models in Gibbs ensemble phase equilibria simulations of the H_2S–pentane mixture*, Mol. Phys. 98 (2000), pp. 1895–1905.
[7] G. Kamath, N. Lubna, and J.J. Potoff, *Effect of partial charge parametrization on the fluid phase behavior of hydrogen sulfide*, J. Chem. Phys. 123 (2005), 124505.
[8] S.K. Nath and J.J. de Pablo, *Simulation of vapour–liquid equilibria for branched alkanes*, Mol. Phys. 98 (2000), pp. 231–238.
[9] S.K. Nath, F.A. Escobedo, and J.J. de Pablo, *On the simulation of vapor–liquid equilibria for alkanes*, J. Chem. Phys. 108 (1998), pp. 9905–9907.
[10] P. Ungerer, C. Beauvais, J. Delhommelle, A. Boutin, B. Rousseau, and A.H. Fuchs, *Optimization of the anisotropic united atoms intermolecular potential for n-alkanes*, J. Chem. Phys. 112 (2000), pp. 5499–5510.
[11] M.G. Martin and J.I. Siepmann, *Transferable potentials for phase equilibria. 1. United-atom description of n-alkanes*, J. Phys. Chem. B 102 (1998), pp. 2569–2577.
[12] B. Chen, J.J. Potoff, and J.I. Siepmann, *Monte Carlo calculations for alcohols and their mixtures with alkanes. Transferable potentials for phase equilibria, 5. United-atom description of primary, secondary, and tertiary alcohols*, J. Phys. Chem. B 105 (2001), pp. 3093–3104.
[13] S. Toxvaerd, *Equation of state of alkanes II*, J. Chem. Phys. 107 (1997), pp. 5197–5204.
[14] B. Smit, S. Karaborni, and J.I. Siepmann, *Computer simulations of vapor–liquid phase equilibria of n-alkanes*, J. Chem. Phys. 102 (1995), pp. 2126–2140.
[15] J.M. Stubbs, J.J. Potoff, and J.I. Siepmann, *Transferable potentials for phase equilibria. 6. United-atom description for ethers, glycols, ketones, and aldehydes*, J. Phys. Chem. B 108 (2004), pp. 17596–17605.
[16] J. Delhommelle, C. Tschirwitz, G. Granucci, P. Millie, D. Pattou, and A.H. Fuchs, *Derivation of an optimized potential for phase equilibria (OPPE) for sulfides and thiols*, J. Phys. Chem. B 104 (2000), pp. 4745–4753.
[17] M. Mezei, *A cavity-biased (T, V, mu) Monte Carlo method for computer simulation of fluids*, Mol. Phys. 40 (1980), pp. 901–906.
[18] J. Siepmann and D. Frenkel, *Configurational-bias Monte Carlo – A new sampling scheme for flexible chains*, Mol. Phys. 75 (1992), pp. 59–70.
[19] S.T. Cui, P.T. Cummings, and H.D. Cochran, *Configurational bias Gibbs ensemble Monte Carlo simulation of vapor–liquid equilibria of linear and short-branched alkanes*, Fluid Phase Equilib. 141 (1997), pp. 45–61.
[20] N.D. Zhuravlev and J.I. Siepmann, *Exploration of the vapour–liquid phase equilibria and critical points of triacontane isomers*, Fluid Phase Equilib. 134 (1997), pp. 55–61.
[21] B. Neubauer, J. Delhommelle, A. Boutin, B. Tavitian, and A.H. Fuchs, *Monte Carlo simulations of squalane in the Gibbs ensemble*, Fluid Phase Equilib. 155 (1999), pp. 167–176.
[22] N.D. Zhuravlev, M.G. Martin, and J.I. Siepmann, *Vapor–liquid phase equilibria of triacontane isomers: Deviations from the principle of corresponding states*, Fluid Phase Equilib. 202 (2002), pp. 307–324.

[23] M.D. Macedonia and E.J. Maginn, *A biased grand canonical Monte Carlo method for simulating adsorption using all-atom and branched united atom models*, Mol. Phys. 96 (1999), pp. 1375–1390.
[24] J.K. Singh and J.R. Errington, *Calculation of phase coexistence properties and surface tensions of n-alkanes with grand-canonical transition-matrix Monte Carlo simulation and finite-size scaling*, J. Phys. Chem. B 110 (2006), pp. 1369–1376.
[25] A.S. Paluch, V.K. Shen, and J.R. Errington, *Comparing the use of Gibbs ensemble and grand-canonical transition-matrix Monte Carlo methods to determine phase equilibria*, Ind. Eng. Chem. Res. 47 (2008), pp. 4533–4541.
[26] F.G. Wang and D.P. Landau, *Determining the density of states for classical statistical models: A random walk algorithm to produce a flat histogram*, Phys. Rev. E 64 (2001), 056101.
[27] F.G. Wang and D.P. Landau, *Efficient multiple range random walk algorithm to calculate density of states*, Phys. Rev. Lett. 86 (2001), pp. 2050–2053.
[28] N.A. Wilding, *Computer simulation of fluid phase transitions*, Am. J. Phys. 69 (2001), pp. 1147–1161.
[29] M.S. Shell, P.G. Debenedetti, and A.Z. Panagiotopoulos, *Generalization of the Wang–Landau method for off-lattice simulations*, Phys. Rev. E 66 (2002), 056703.
[30] M.S. Shell, P.G. Debenedetti, and A.Z. Panagiotopoulos, *An improved Monte Carlo method for direct calculation of the density of states*, J. Chem. Phys. 119 (2003), pp. 9406–9411.
[31] J.J. de Pablo, Q. Yan, and R. Faller, *Density-of-states Monte Carlo method for simulation of fluids*, J. Chem. Phys. 116 (2002), pp. 8649–8659.
[32] C. Desgranges and J. Delhommelle, *Phase equilibria of molecular fluids via hybrid Monte Carlo Wang–Landau simulations: Applications to benzene and n-alkanes*, J. Chem. Phys. 130 (2009), 244109.
[33] G. Ganzenmuller and P.J. Camp, *Applications of Wang–Landau sampling to determine phase equilibria in complex fluids*, J. Chem. Phys. 127 (2007), 154504.
[34] T. Aleksandrov, C. Desgranges, and J. Delhommelle, *Vapor–liquid equilibria of copper using hybrid Monte Carlo Wang–Landau simulations*, Fluid Phase Equilib. 287 (2010), pp. 79–83.
[35] C. Desgranges, J.M. Hicks, A. Magness, and J. Delhommelle, *Phase equilibria of polyaromatic hydrocarbons by hybrid Monte Carlo Wang–Landau simulations*, Mol. Phys. 108 (2010), pp. 151–158.
[36] C. Desgranges and J. Delhommelle, *Molecular insight into the pathway to crystallization of aluminum*, J. Am. Chem. Soc. 129 (2007), pp. 7012–7013.
[37] C. Desgranges and J. Delhommelle, *Molecular simulation of the crystallization of aluminum from the supercooled liquid*, J. Chem. Phys 127 (2007), 144509.
[38] C. Desgranges and J. Delhommelle, *Polymorph selection during the crystallization of softly-repulsive spheres: The inverse power law potential*, J. Phys. Chem. B 111 (2007), pp. 12257–12262.
[39] C. Desgranges and J. Delhommelle, *Crystallization mechanisms for xenon at high pressure and high temperature*, Phys. Rev. B 77 (2008), 054201.
[40] C. Desgranges and J. Delhommelle, *Molecular simulation of the nucleation and growth of gold nanoparticles*, J. Phys. Chem. C 113 (2009), pp. 3607–3611.
[41] S. Duane, A.D. Kennedy, B.J. Pendleton, and D. Roweth, *Hybrid Monte Carlo*, Phys. Lett. B 195 (1987), pp. 216–222.
[42] B. Mehlig, D.W. Heerman, and B.M. Forrest, *Hybrid Monte Carlo method for condensed-matter systems*, Phys. Rev. B 45 (1992), pp. 679–685.
[43] G.J. Martyna, M.E. Tuckerman, D.J. Tobias, and M.L. Klein, *Explicit reversible integrators for extended systems dynamics*, Mol. Phys. 87 (1996), pp. 1117–1157.
[44] J.S. Rowlinson and F.L. Swinton, *Liquids and Liquid Mixtures*, Butterworths, London, 1982.
[45] J. Delhommelle, A. Boutin, B.A. Tavitian, A.D. Mackie, and A.H. Fuchs, *Vapour–liquid coexistence curves of the united-atom and anisotropic united-atom force fields for alkane mixtures*, Mol. Phys. 96 (1999), pp. 1517–1524.
[46] M.P. Allen and D.J. Tildesley, *Computer Simulation of Liquids*, Clarendon, Oxford, 1987.
[47] J. Delhommelle and P. Millie, *Inadequacy of the Lorentz–Berthelot combining rules for accurate predictions of equilibrium properties by molecular simulation*, Mol. Phys. 99 (2001), pp. 619–625.
[48] N.B. Vargaftik, Y.K. Vinoradov, and V.S. Yargin, *Handbook of Physical Properties of Liquids and Gases*, Begell House, New York, 1996.